Possible Intermediates in Biological Metalloporphyrin Oxidative Degradation. Nickel, Copper, and Cobalt Complexes of Octaethylformybiliverdin and Their Conversion to a Verdoheme

Richard Koerner, Marilyn M. Olmstead, Andrzej Ozarowski, Shane L. Phillips, Pamela M. Van Calcar, Krzysztof Winkler,† and Alan L. Balch*

Contribution from the Department of Chemistry, University of California, Davis, California 95616

Received September 2, 1997

Abstract: Formylbiliverdin and related chlorophyll-derived molecules are possible products of heme catabolism and other biologically important oxidative processes and are likely to be initially formed as metal complexes. To explore the properties of the formylbiliverdin moiety bound to transition metal ions, complexes of octaethylformylbiliverdin (H_2OEFB) with Cu(II), Ni(II), and Co(II) have been prepared, since attempts to prepare an iron complex have produced only an unstable material. Transmetalation of Mg^{II}(OEFB), made by photooxidation of Mg^{II}(octaethyl-porphyrin), with a metal(II) acetate yields the low-spin complexes: Cu^{II}(OEFB), Ni^{II}(OEFB), and Co^{II}(OEFB). Single-crystal X-ray diffraction of Cu^{II}(OEFB) reveals that it consists of a four-coordinate copper(II) center which is bound to the four nitrogen atoms in distorted planar coordination. The tetrapyrrole ligand has a helical geometry. The structure of the solid is complicated by the existence of three molecules in the asymmetric unit and C−H···O hydrogen bonding between pairs of these in the tab/slot arrangement seen in complexes of octaethylbiliverdin. Both Cu^{II}(OEFB) and Co^{II}(OEFB) can be converted to the verdoheme analogues, $[Cu^{II}(OEOP)]^+$ and $[Co^{II}(OEOP)]^+$, where OEOP is the anion of octaethyl-5-oxaporphyrin, by the addition of hydrogen peroxide. Additionally, $[Cu^{II}(OEOP)]^+$ can be produced by heating a toluene solution Cu^{II}(OEFB) in the presence of trifluoroacetic acid under dioxygen. Carbon monoxide is produced when Cu^{II}(OEFB) is converted to $[Cu^{II}(OEOP)]^+$ by either method. $[Cu^{II}(OEOP)](PF_6)$ has been characterized by single-crystal X-ray diffraction which shows that the cation has a planar, porphyrin-like structure. The room-temperature EPR spectrum of this complex shows that the copper is four-coordinate with four nitrogen based ligands, but frozen solutions of $[Cu^{II}(OEOP)]^+$ show a triplet EPR spectrum indicative of a dimeric species much like that in the X-ray crystal structure. The ^{1}H NMR spectrum of diamagnetic Ni^{II}(OEFB) has been shown to be consistent with the helical structure through the use of lanthanide and chiral lanthanide shift reagents. The EPR spectra of Co^{II}(OEFB) show that it forms a low-spin adduct with pyridine and that this adduct acts as a reversible dioxygen carrier. The geometric and electronic structural properties of these complexes of formylbiliverdin are compared to those of analogous compounds of biliverdin and of porphyrins.

Introduction

Heme catabolism catalyzed by heme oxygenase results in the remarkable activation of dioxygen that cleaves one C−H and two C−C bonds in heme as shown for the transformation of heme, **1**, to verdoheme, **2**, in Scheme 1.[1] Verdoheme, the diamagnetic iron(II) complex of 5-oxaporphyrin,[2] is a spectroscopically detected intermediate, which is subsequently converted into biliverdin.[3−7] The enzyme is specific for cleavage at the α-meso position. The carbon atom at that meso site is eliminated as carbon monoxide. Details of the reactions involved in this process are limited although there is consensus that the initial stage involves meso-hydroxylation (i.e., C−H bond activation).[4] Further reaction could involve stepwise fragmentation of the adjacent C−C bonds, and this procedure might result in the intermediate formation of an iron complex of formylbiliverdin, **3a**. Indeed, there are reports that some heme oxygenases yield formylbiliverdin rather than biliverdin as their product.[5] Additionally, a related cleavage of a

Scheme 1

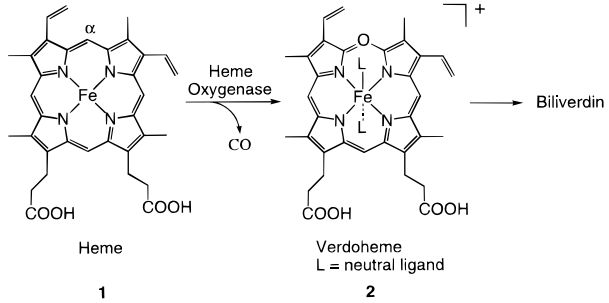

† On leave from the Institute of Chemistry, University of Warsaw, Bialystok Branch, Poland.

(1) Maines, M. D. *Heme Oxygenase: Clinical Applications and Functions*; CRC Press: Boca Raton, FL, 1992. Bissell, D. M. In *Liver: Normal Function and Disease. Bile Pigments and Jaundice*; Ostrow, J. D., Ed.; Marcel Dekker, Inc.: New York, 1986; Vol. 4, p 133.

(2) Balch, A. L.; Koerner, R.; Olmstead, M. M. *J. Chem. Soc., Chem. Commun.* **1995**, 873.

(3) Wilks, A.; Ortiz de Montellano, P. R. *J. Biol. Chem.* **1993**, *268*, 22357.

(4) Wilks, A.; Torpey, J.; Ortiz de Montellano, P. R. *J. Biol. Chem.* **1994**, *269*, 29553.

(5) Nakajima, H. *J. Biol. Chem.* **1963**, *238*, 3797. Nakajima, O.; Gray, C. H. *Biochem. J.* **1967**, *104*, 20.

(6) Iturraspe, J.; Moyano, N.; Frydman, B. *J. Org. Chem.* **1995**, *60*, 6664.

(7) Yokosuka, O.; Billing, B. *Biochim. Biophys. Acta* **1987**, *923*, 268. Furhop, J.-H.; Mauzerall, D. *Photochem. Photobiol.* **1971**, *13*, 453.

S0002-7863(97)03088-6 CCC: $15.00 © 1998 American Chemical Society
Published on Web 01/30/1998

chlorophyll to yield a formyl-terminated tetrapyrrole has been found in senescent tree leaves.[6] This article is concerned with the coordination of the model compound octaethylformylbiliverdin, H_2OEFB, **3b**,[7,8] to transition metal ions in order to explore several aspects of the behavior of this ligand. (1) What types of geometry will this linear tetrapyrrole ligand adopt when coordinated? (2) How do the properties of the complexes of

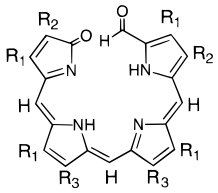

3a R_1 = methyl, R_2 = vinyl
R_3 = propionate

3b $R_1 = R_2 = R_3$ = ethyl
H_2OEFB

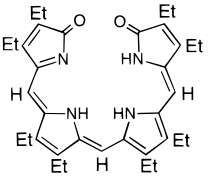

4
H_3OEB

octaethylformylbiliverdin, **3b**, compare with those of the closely related octaethylbiliverdin, **4**, H_3OEB? (3) What is the chemical reactivity of metal complexes of octaethylformylbiliverdin and how does that reactivity relate to heme catabolism? The question of conversion of the formylbiliverdin ligand into the oxaporphyrin (verdoheme) ligand is especially significant in this regard.

Octaethylformylbiliverdin is synthetically accessible through the photooxygenation of Mg^{II}(OEP).[8] However, in regard to question 1 above, the coordination chemistry of this ligand has received limited attention.[9,10] Two zinc complexes have been prepared and crystallographically characterized.[10] The dimeric complex, $\{Zn^{II}(OEFB)\}_2$, **5**, has a structure in which each metal

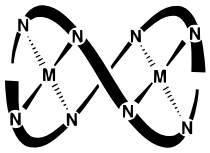

5

is tetrahedrally coordinated by two nitrogen atoms from adjacent pyrrole rings on the two different ligands. Mononuclear (H_2O)-Zn^{II}(OEFB) has a five-coordinate structure.

In regard to question 2 above, octaethylbiliverdin (octaethylbilindione) is known to form complexes in which the tetrapyrrole ligand assumes a helical geometry which is dictated by the need of the two terminal lactam functions to overlap one another when the four pyrrole nitrogen atoms are coordinated to a metal ion of the size of a typical transition metal.[11−17] With Fe(III) and Mn(III), five-coordinate dimers form in which one of the oxygen atoms of each of the tetrapyrroles serves as a ligand toward the metal that is coordinated by four of the nitrogen atoms from the adjacent tetrapyrrole.[11,13] The four-coordinate complexes Co(OEB), Ni(OEB), and Cu(OEB) have helical structures and unusual physical properties that reflect remarkable electronic structures.[11,13,14] For example, Cu(OEB) has magnetic moment of 2.7 μ_B, a readily observed ^{1}H NMR spectrum, and no detectable EPR spectrum (under conditions where a copper(II) complex would produce an easily observable EPR spectrum).[14] Thus, this complex has been formulated with the electronic distribution, $Cu^{II}(OEB^{\bullet})$, with two paramagnetic centers, the copper(II) ion, and the biliverdin radical dianion. These four-coordinate complexes also undergo a series of one-electron transfer reactions which have been thoroughly documented for Co(OEB).[16,17] Additionally, octaethylbiliverdin itself undergoes a two-electron oxidation, and the product of that oxidation has been isolated and characterized by single-crystal X-ray diffraction.[18]

Results

Attempts to insert iron into octaethylformylbiliverdin have produced complexes that have limited stability and are difficult to characterize. To work with more robust complexes, we have turned to copper, nickel, and cobalt where, as expected from the Irving−Williams trends in stability, the complexes are more readily prepared and isolated.

Synthesis and Characterization of Cu^{II}(OEFB). Photooxidation of Mg^{II}(OEP) to the magnesium octaethylformylbiliverdin complex followed by transmetalation by $Cu^{II}(OAc)_2 \cdot H_2O$ produces octaethylformylbiliverdin copper(II), Cu^{II}(OEFB), **6**, in ca. 22% yield. The dark black air stable solid

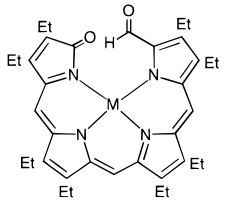

6
M^{II}(OEFB), M = Cu, Ni, Co

is soluble in chlorinated and aromatic solvents to produce a brown-orange solution. The solid is insoluble in *n*-hexane. The electronic absorption spectrum of Cu^{II}(OEFB) in methylene chloride is shown in trace A of Figure 1. The EPR spectrum of Cu^{II}(OEFB) is similar to that reported earlier.[19] No ^{1}H NMR spectrum was detectable for Cu^{II}(OEFB).

Crystal and Molecular Structure of Cu^{II}(OEFB). Cu^{II}(OEFB) crystallizes with three independent molecules in the asymmetric unit. Figure 2 shows a perspective view of the asymmetric unit (ethyl groups have been omitted for clarity), while Figure 3 shows a perspective view of a single molecule of Cu^{II}(OEFB). The other two molecules have nearly identical geometries. Important bond lengths and angles are listed in Table 1.

The copper complexes have four-coordinate geometry with Cu−N distances which are slightly shorter than the correspond-

(8) Wasser, P. K. W.; Fuhrhop, J.-H. *Ann. N. Y. Acad. Sci.* **1973**, *206*, 533.
(9) Fuhrhop, J.-H.; Wasser, P. K. W.; Subramanian, J.; Schrader, U. *Liebigs Ann. Chem.* **1974**, 1450.
(10) Struckmeier, G.; Thewalt, U.; Fuhrhop, J.-H. *J. Am. Chem. Soc.* **1976**, *98*, 278.
(11) Bonnett, R.; Buckley, D. G.; Hamzetash, D. *J. Chem. Soc., Perkin Trans I* **1981**, 322.
(12) *(12)* Bonfiglio, J. V.; Bonnett, R.; Buckley, D. G.; Hamzetash, D.; Hursthouse, M. B.; Abdul Malik, K. M.; McDonagh, A. F.; Trotter, J. *Tetrahedron* **1983**, *39*, 1865.
(13) Balch, A. L.; Latos-Grażyński, L.; Noll, B. C.; Olmstead, M. M.; Safari, N. *J. Am. Chem. Soc.* **1993**, *115*, 9056.
(14) Balch, A. L.; Mazzanti, M.; Noll, B. C.; Olmstead, M. M. *J. Am. Chem. Soc.* **1993**, *115*, 12206.
(15) Balch, A. L.; Mazzanti, M.; Noll, B. C.; Olmstead, M. M. *J. Am. Chem. Soc.* **1994**, *116*, 9114.
(16) Attar, S.; Balch, A. L.; Van Calcar, P. M.; Winkler, K. *J. Am. Chem. Soc.* **1997**, *119*, 3317.
(17) Attar, S.; Ozarowski, A.; Van Calcar, P. M.; Winkler, K.; Balch, A. L. *Chem. Commun.* **1997**, 1115.
(18) Balch, A. L.; Koerner, R.; Olmstead, M. M.; Mazzanti, M.; Safari, N.; St. Claire, T. *J. Chem. Soc., Chem. Commun.* **1995**, 643.
(19) Subramanian, J.; Fuhrhop, J.-H.; Salek, A.; Gossauer, A. *J. Magn. Reson.* **1974**, *15*, 19.

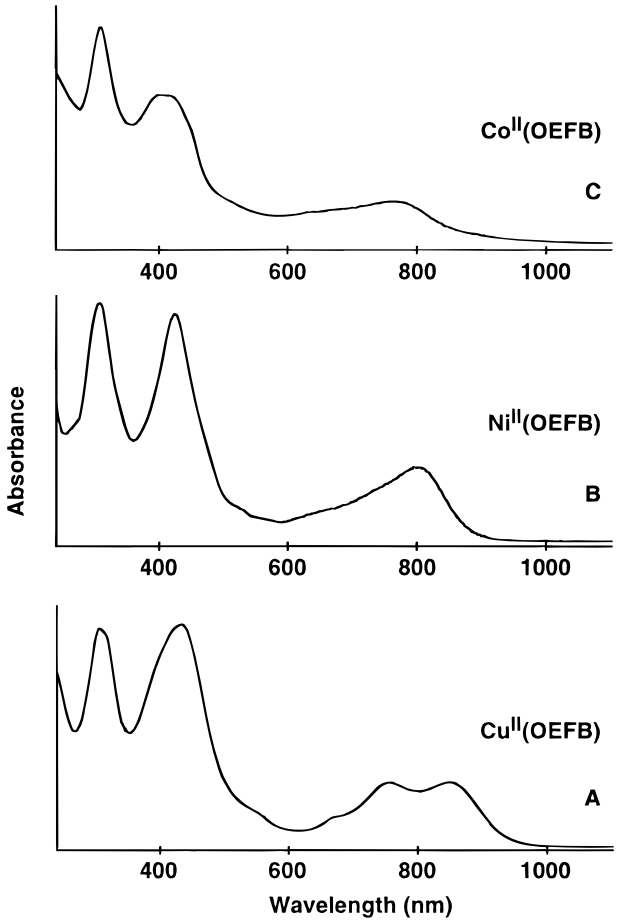

Figure 1. Electronic absorption spectra [λ_{max}, nm (ϵ, $cm^{-1}\cdot L\cdot mol^{-1}$)] of methylene chloride solutions: A, Cu^{II}(OEFB) 308 (3.8×10^4), 432 (3.9×10^4), 752 (1.0×10^4), 844 (1.0×10^4); B, Ni^{II}(OEFB) 308 (2.9×10^4), 424 (2.8×10^4), 802 (9.2×10^3); C, Co^{II}(OEFB) 310 (2.6×10^4), 400 (2×10^4), 766 (5.4×10^3).

ing distances in copper(II) porphyrins.[20] The Cu−N distances that involve the pyrrole ring which is attached to the formyl group fall in the narrow range, 1.973−1.971 Å, and are systematically longer than the other Cu−N distances which are in the range, 1.939−1.957(2) Å. All three independent molecules have helical structures in which the formyl group at one end of the tetrapyrrole ligand lies above (or below) the lactam group at the opposite end of the ligand. Due to the overlapping of these end groups, the copper coordination geometry is restricted from planarity, yet is not tetrahedral. Thus, the pseudo-trans angles (i.e., those corresponding to N(1)−Cu(1)−N(3) and N(2)−Cu(1)−N(4)) fall in the range, 155.86(10)−159.35(10)°, while the pseudo-cis angles within the six-membered chelate rings are in the range, 89.96(10)−96.29(10)°. Within the asymmetric unit seen in Figure 2, the complex that contains Cu(1) has the P helical conformation, while complexes that contain Cu(2) and Cu(3) are both in the M helical conformation. However, the solid contains a racemic mixture of helical Cu^{II}(OEFB) complexes, since there is a center of symmetry in the space group that generates the other enantiomers.

The three independent Cu^{II}(OEFB) molecules are similar in structure to copper octaethylbiliverdin, Cu^{II}(OEB$^{\bullet}$), which was previously characterized by single-crystal X-ray diffraction. Figure 4 shows an overlay comparison of Cu^{II}(OEFB) (solid structure) and Cu^{II}(OEB) (dashed structure). The greatest

(20) Scheidt, R. W.; Reed, C. A. *Chem. Rev.* **1981**, *81*, 543.

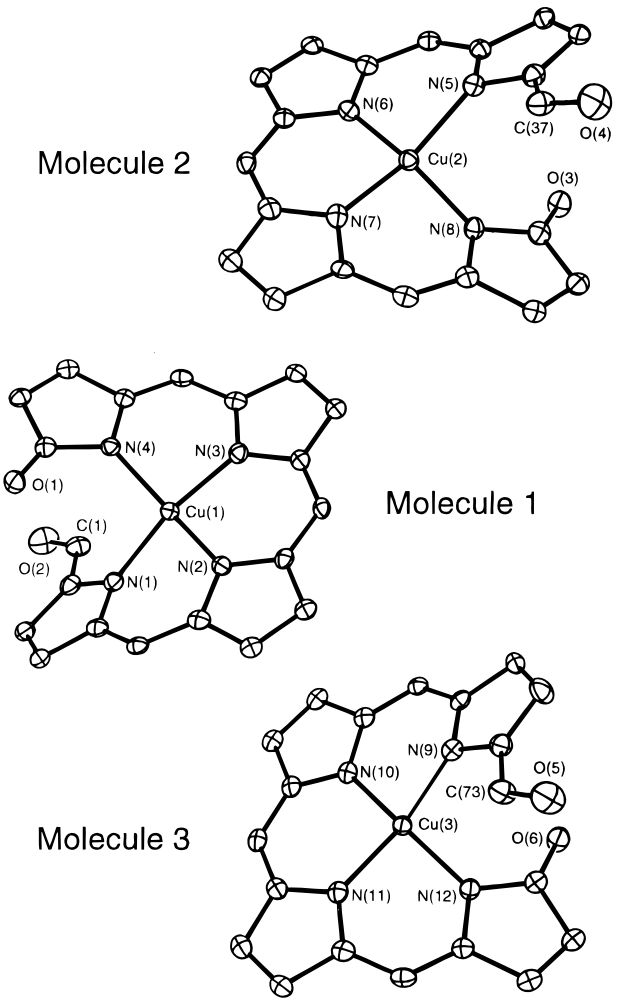

Figure 2. Perspective view of the asymmetric unit of Cu^{II}(OEFB) with 50% thermal contours for all atoms. The ethyl groups have been omitted for clarity. Relevant metrical parameters are listed in Table 1.

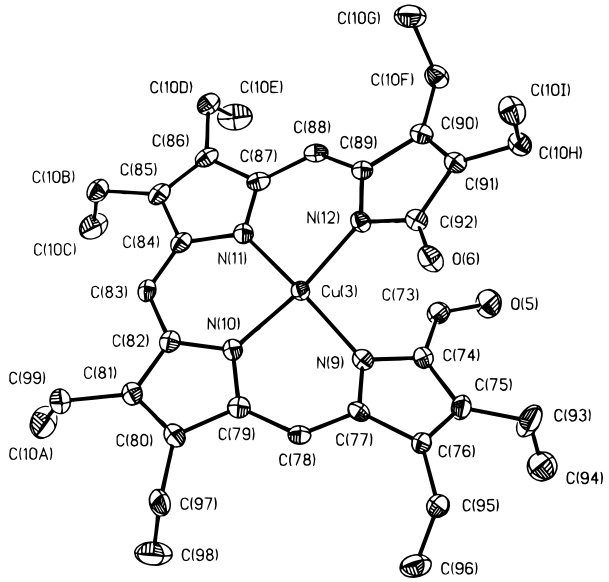

Figure 3. Perspective view of one of the Cu^{II}(OEFB) complexes with 50% thermal contours for all atoms.

difference is seen in the pyrrole ring of Cu^{II}(OEFB) which is substituted with the formyl group, while the other terminal pyrrole ring shows a somewhat smaller inward displacement.

Analysis of the Hydrogen Bonding Network in Cu^{II}(OEFB). Analysis of the molecular packing in Cu^{II}(OEFB)

Scheme 2. Crystal Packing within Cu^{II}((oefb)

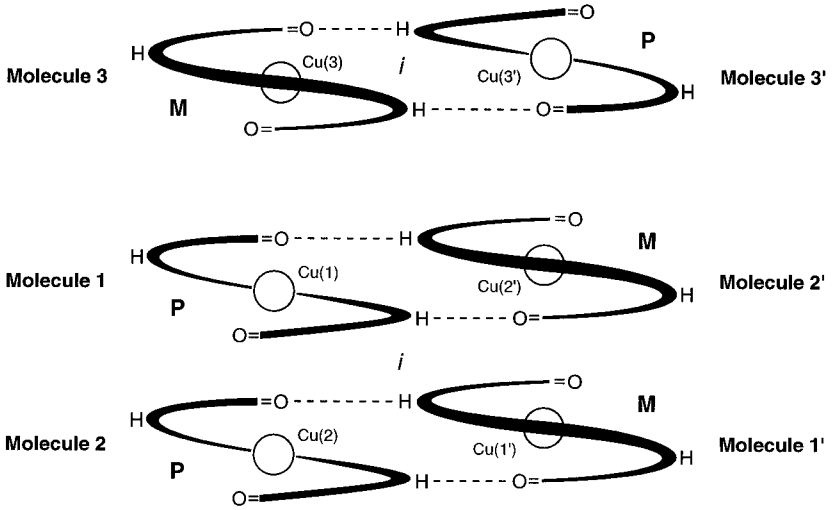

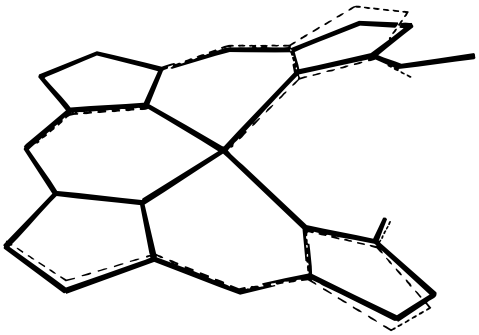

Figure 4. An overlay comparison of the structures of the cores of Cu^{II}(OEFB) (solid lines) and Cu^{II}(OEB•) (dashed lines).

Table 1. Selected Bond Lengths (Å) and Angles (deg) for Cu^{II}(OEFB)

Bond Lengths (Å)					
Cu(1)−N(1)	1.973(2)	Cu(2)−N(5)	1.972(2)	Cu(3)−N(9)	1.971(3)
Cu(1)−N(2)	1.940(2)	Cu(2)−N(6)	1.945(2)	Cu(3)−N(10)	1.939(2)
Cu(1)−N(3)	1.956(2)	Cu(2)−N(7)	1.957(3)	Cu(3)−N(11)	1.952(2)
Cu(1)−N(4)	1.948(2)	Cu(2)−N(8)	1.944(2)	Cu(3)−N(12)	1.942(2)
O(2)−C(1)	1.214(4)	O(4)−C(37)	1.215(4)	O(5)−C(73)	1.220(4)
C(1)−C(2)	1.446(5)	C(37)−C(38)	1.450(4)	C(73)−C(74)	1.450(5)
O(1)−C(20)	1.225(4)	O(3)−C(56)	1.220(4)	O(6)−C(92)	1.218(4)

Bond Angles (deg)			
N(2)−Cu(1)−N(4)	158.40(10)	N(2)−Cu(1)−N(3)	91.91(10)
N(4)−Cu(1)−N(3)	90.29(10)	N(2)−Cu(1)−N(1)	90.21(10)
N(4)−Cu(1)−N(1)	95.84(10)	N(3)−Cu(1)−N(1)	157.65(10)
O(1)−C(20)−C(19)	126.2(3)	O(1)−C(20)−N(4)	125.7(3)
O(2)−C(1)−C(2)	126.9(3)		
N(8)−Cu(2)−N(6)	159.35(10)	N(8)−Cu(2)−N(7)	89.96(10)
N(6)−Cu(2)−N(7)	92.49(10)	N(8)−Cu(2)−N(5)	95.63(10)
N(6)−Cu(2)−N(5)	90.00(10)	N(7)−Cu(2)−N(5)	157.18(10)
O(3)−C(56)−C(55)	126.3(3)	O(3)−C(56)−N(8)	125.5(3)
O(4)−C(37)−C(38)	126.7(3)		
N(10)−Cu(3)−N(12)	157.70(10)	N(10)−Cu(3)−N(11)	92.29(10)
N(12)−Cu(3)−N(11)	90.04(10)	N(10)−Cu(3)−N(9)	90.58(10)
N(12)−Cu(3)−N(9)	96.29(10)	N(11)−Cu(3)−N(9)	155.86(10)
O(6)−C(92)−C(91)	126.4(3)	O(6)−C(92)−N(12)	125.6(3)
O(5)−C(73)−C(74)	126.4(3)		

indicates that a C−H···O hydrogen bonding scheme that is similar to those seen in metal complexes of octaethylbilindione[16] is present in this solid as well. This scheme utilizes the tab/slot motif shown schematically at the top of Table 2. The lactam group of the Cu^{II}(OEFB) ligand interacts with one meso C−H group and two methylene C−H bonds on adjacent ethyl groups of a second molecule of the complex as seen in Figure 5. Thus each molecule crystallizes as part of a dimer that is connected

Table 2. O···H−C Distances and Angles in Cu^{II}(OEFB)

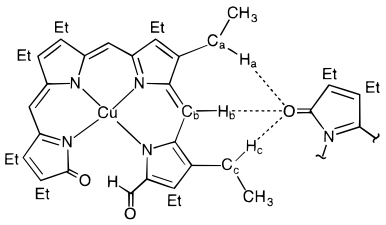

	molecule 1[a§]	molecule 2[a§]	molecule 3[a§]
	Distance (Å)		
O−Ha	2.880	2.626	2.694
O−Hb	2.432	2.377	2.405
O−Hc	2.585	2.627	2.567
O−Ca	3.660	3.546	3.588
O−Cb	3.379	3.333	3.359
O−Cc	3.363	3.336	3.310
	Angle (deg)		
O−Ha−Ca	139.0	160.7	166.0
O−Hb−Cb	169.0	174.2	172.3
O−Hc−Cc	138.2	131.0	134.4

[a] The molecule number refers to the numbering given to the copper atom in each molecule.

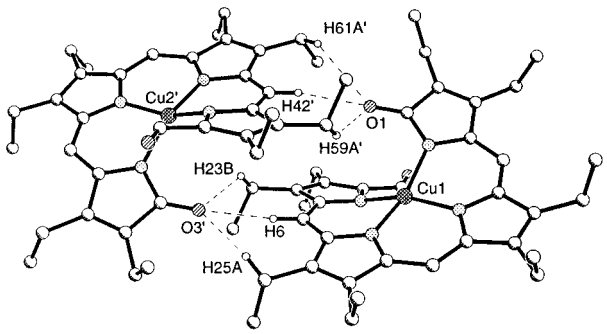

Figure 5. A view of the hydrogen bonding pairing of molecule 1 and molecule 2′.

by a pair of the tab/slot motifs shown at the top of Table 2. Because there are three independent molecules in the solid, this pairing, which is shown in Scheme 2, is complex. The hydrogen bonding interaction between molecule 3 (which contains Cu(3)) and its enantiomer, molecule 3′, occurs across an inversion center. Similarly, molecule 1 (Cu(1)) interacts with molecule 2′ (Cu(2′)), the symmetry generated enantiomer of molecule 2, as shown in Figure 5. The center of symmetry generates a

Table 3. Selected Bond Lengths (Å) and Angles (deg) for $[Cu^{II}(OEOP)](PF_6)\cdot CH_2Cl_2$[a]

Bond Lengths (Å)					
Cu−N(1)	1.977(3)	Cu−N(2)	1.970(3)	Cu−N(3)	1.977(3)
Cu−N(4)	1.982(3)	Cu−N(4′)	3.250(4)	O−C(1)	1.348(4)
O−C(19)	1.353(4)	C(4)−C(5)	1.367(5)	C(5)−C(6)	1.395(5)
C(9)−C(10)	1.383(5)	C(10)−C(11)	1.380(5)	C(14)−C(15)	1.402(5)
C(15)−C(16)	1.364(5)	Cu−Cu′	3.571(2)		

Bond Angles (deg)			
N(1)−Cu−N(2)	90.48(11)	N(1)−Cu−N(3)	177.49(12)
N(2)−Cu−N(3)	91.77(11)	N(1)−Cu−N(4)	87.47(11)
N(2)−Cu−N(4)	177.92(12)	N(3)−Cu−N(4)	90.27(11)
N(1)−Cu−N(4′)	91.7(1)	N(2)−Cu−N(4′)	82.8(1)
N(3)−Cu−N(4′)	89.7(1)	N(4)−Cu−N(4′)	97.7(1)
C(1)−O−C(19)	124.6(3)		

[a] Symmetry code: ′ = $-x,-y,1-z$..

second hydrogen bonded pair made up of molecule 1′ and molecule 2 as shown in Scheme 2. Interatomic distances for these interactions are given in Table 2. The interatomic distances are comparable to those found in related hydrogen bonded structures in which OEB is the ligand.[16]

Preparation of the Copper Verdoheme Analogue, $[Cu^{II}(OEOP)]^+$. The copper verdoheme analogue, $[Cu^{II}(OEOP)]^+$, has been obtained by three methods from either Cu^{II}(OEFB) or Cu^{II}(OEP). Treatment of a toluene solution of Cu^{II}(OEFB) with dioxygen in the presence of trifluoroacetic acid produces blue-green $[Cu^{II}(OEOP)](O_2CCF_3)$ in 56% yield as shown in eq 1.

(1) 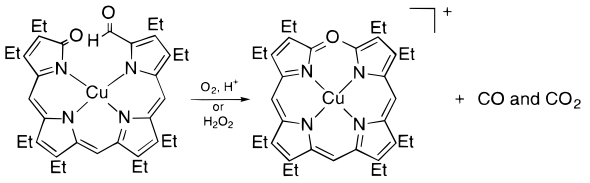

The addition of hydrogen peroxide to a dichloromethane solution of Cu^{II}(OEFB) followed by anion metathesis with ammonium hexafluorophosphate produces $[Cu^{II}(OEOP)](PF_6)$ in 84% yield. In both of these reactions, carbon monoxide as well as carbon dioxide have been detected as additional products by infrared analysis of the gases in the sealed reaction vessel. The addition of hydrogen peroxide to a dichloromethane solution of Cu^{II}(OEP) results in the isolation of $[Cu^{II}(OEOP)](PF_6)$ after the addition of ammonium hexafluorophosphate, but the yield is poor, 2%. The spectroscopic properties of the cations produced in all three reactions are identical. The UV/vis spectrum shows a typical verdoheme-like pattern with intense, low energy features at 622 and 666 nm.

Crystal and Molecular Structure of $[Cu^{II}(OEOP)](PF_6)\cdot CH_2Cl_2$. The blue-green salt crystallizes with one cation, one anion, and a dichloromethane cosolvate in the asymmetric unit. Selected bond distances and angles for the cation are listed in Table 3. The upper part of Figure 6 shows a drawing of the cation, which consists of the planar 5-oxaporphyrin macrocyclic core with a four-coordinate, planar copper(II) ion at its center. The hexafluorophosphate anion does not interact with the cation. The Cu−N distances, which have an average bond length of 1.977 Å, are similar to the corresponding bond distances in copper porphyrins.[20] As usual with 5-oxaporphyrin complexes,[2,21−23] there is disorder in the location of the oxygen atom which is fractionally distributed over two "trans" meso

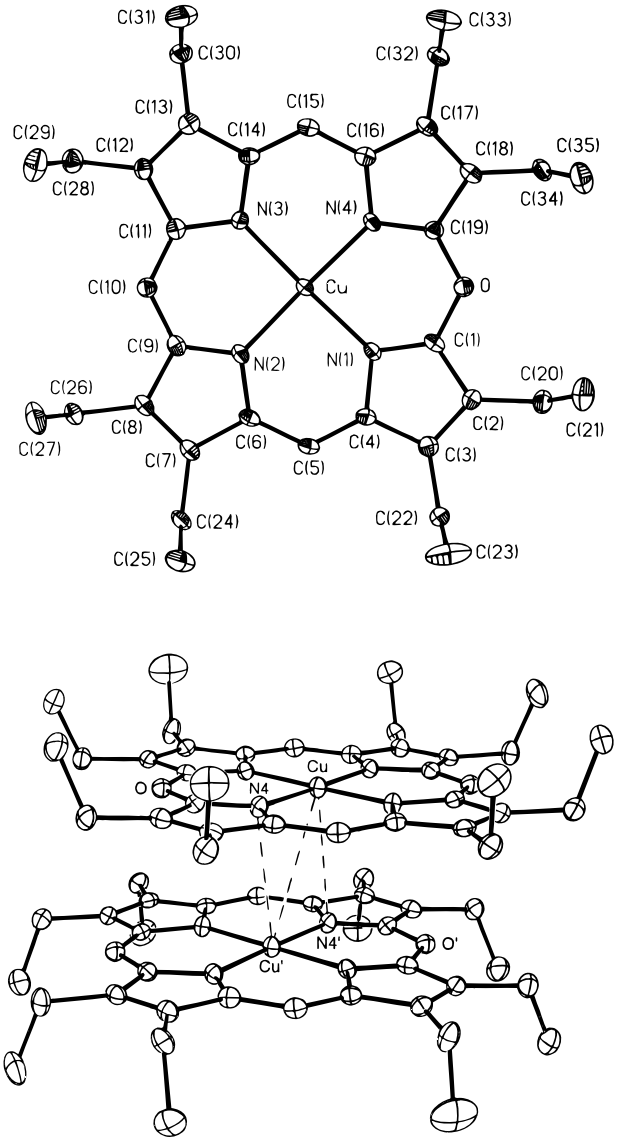

Figure 6. The upper part of the figure shows a perspective view the cation in $[Cu^{II}(OEFB)](PF_6)\cdot CH_2Cl_2$ with 50% thermal contours for all atoms. The oxygen atom is disordered over two sites, with the minor site of occupancy being identical to the position of C(10). The lower part of the figure shows the cofacial dimer formed by two $[Cu^{II}(OEFB)]$ cations. The dashed lines illustrate the nonbonding Cu···N4′ and Cu···Cu′ interactions. The Cu···N4′ distance is 3.250(4) Å, while the Cu···Cu′ distance is 3.571(2) Å. Other relevant metrical parameters are listed in Table 3.

positions with an occupancy at one site of 0.919(10) and 0.081(10) at the other. The core of the 5-oxaporphyrin complex is quite planar, with an average mean plane displacement of 0.022 Å. As shown in the lower part of Figure 6, the cations form cofacial dimers with nonbonding interactions between Cu and N4′ (the center of symmetry generated equivalent to N4). N4′ shows a mean plane displacement of 0.056 Å toward Cu. The Cu···N4′ distance is 3.250(4) Å with an N4−Cu−N4′ angle of 97.7°. Within the dimer the distance between the two 5-oxaporphyrin planes averages 3.30 Å, and the Cu···Cu separation is 3.571(2) Å.

EPR Studies of $[Cu^{II}(OEOP)]^+$. At room temperature the EPR spectrum of $[Cu^{II}(OEOP)]^+$ shows a typical pattern for a copper(II) tetrapyrrole complex and is shown in trace A of Figure 7. Simulation of this spectrum yielded the following

(21) Balch, A. L.; Latos-Grażyński, L.; Noll, B. C.; Olmstead, M. M.; Szterenberg, L.; Safari, N. *J. Am. Chem. Soc.* **1993**, *115*, 1422.
(22) Balch, A. L.; Noll, B. C.; Safari, N. *Inorg. Chem.* **1993**, *32*, 2901.
(23) Balch, A. L.; Mazzanti, M.; St. Claire, T. N.; Olmstead, M. M. *Inorg. Chem.* **1995**, *34*, 2194.

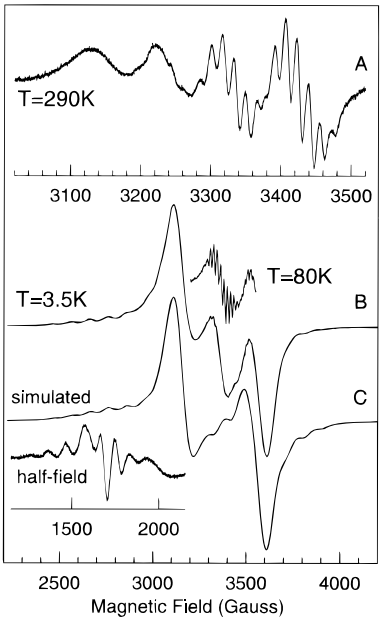

Figure 7. A, the X band EPR spectrum of $[Cu^{II}(OEOP)]^+$ in methylene chloride at 290 K. B, the triplet spectrum of dimeric $[Cu^{II}(OEOP)]^+$ at 3.5 K. The half-field transition is shown in the bottom left part of the figure. C, the simulation of the triplet spectrum in trace B.

isotropic g values and hyperfine coupling constants: $g_{iso} = 2.095$, $A_{iso}(^{63}Cu) = 85.1 \times 10^{-4}$ cm^{-1}, $A_{iso}(^{14}N) = 15.6 \times 10^{-4}$ cm^{-1}.

When a methylene chloride solution of $[Cu^{II}(OEOP)]^+$ is frozen, a spin-triplet spectrum of a dimeric copper compound is clearly observed with a well resolved, seven-line hyperfine structure of two copper nuclei in the parallel part of the $\Delta m_s = 1$ region as well as in the half-field transition. The triplet spectrum is shown in trace B of Figure 7, and a simulation of this spectrum is shown in trace C of Figure 7. The perpendicular part of the triplet spectrum shows no hyperfine structure. Halfway between the perpendicular features of the triplet, a perpendicular line of monomeric $[Cu^{II}(OEOP)]^+$ appears at $g = 2.055$. This line exhibits very sharp nitrogen hyperfine structure except at very low temperatures. Simulation (see Experimental section) of the triplet spectrum at 3.5 K yielded the following parameters: $g_{x,y} = 2.055$, $g_z = 2.175$, $|D| = 430 \times 10^{-4}$ cm^{-1}, $E \sim 0$, $|A_{x,y}(Cu)| \sim 10 \times 10^{-4}$ cm^{-1}, $|A_z(Cu)| = 101.5 \times 10^{-4}$ cm^{-1} and an approximate angle of 10° between the directions of g_{zz} and D_{zz}. No satisfactory simulation was possible with g_{zz} parallel to D_{zz}. The average of $g_{x,y}$ and g_z is equal to g_{iso} from the liquid solution at room temperature, strongly suggesting that the dimer observed in frozen solutions is formed by two $[Cu^{II}(OEOP)]^+$ monomers. Similar triplet EPR spectra have been observed for several monomeric copper(II) porphyrins which dimerize in frozen solution.[24]

From the solution state EPR spectrum of $[Cu^{II}(OEOP)]^+$ the spin density on each nitrogen was found to be 2.6% when the Fermi contact term for nitrogen is taken as 0.0604 cm^{-1}.[25] The value of α^2 for the molecular orbital composed of $d_{x^2-y^2}$ and the σ nitrogen hybrids was calculated to be 0.76.[26] If the A_z(Cu, dimer) component is doubled and substituted for A_z(Cu, monomer), then the value for $A_{x,y}$(Cu, monomer) is calculated to be 26×10^{-4} cm^{-1}. This yields a molecular orbital coefficient of 0.75 for α^2, in agreement with the value calculated from the isotropic parameters for the monomer. Utilizing the metric data from the X-ray crystal structure of $[Cu^{II}(OEOP)](PF_6)\cdot CH_2Cl_2$ as a model for the dimeric species in frozen solution, the dipole−dipole component of the zero-field splitting tensor was calculated.[27] For $\alpha^2 = 1$ and no spin density delocalized onto the nitrogens, the result is $D = -643 \times 10^{-4}$ cm^{-1}, $E = -2 \times 10^{-4}$ cm^{-1}, and a g_{zz}-D_{zz} angle of 25.4°, which is identical to the angle between the Cu···Cu vector and the normal to the plane of four nitrogen atoms measured from the X-ray crystal structure. For $\alpha^2 = 0.76$, where the unpaired spin density is localized on the copper and nitrogen atoms, one finds $D = -502 \times 10^{-4}$ cm^{-1}, $E = 2 \times 10^{-4}$ cm^{-1}, and a g_{zz}-D_{zz} angle of 22°. For $\alpha^2 = 1$ with the spin density delocalized over the four points midway between each copper and nitrogen, the calculated vales were $D = -470 \times 10^{-4}$ cm^{-1}, $E = -2 \times 10^{-4}$ cm^{-1} and a g_{zz}-D_{zz} angle of 20°. This result is in excellent agreement with the experimentally observed values. The difference between the experimentally observed g_{zz}-D_{zz} angle (10°) and the values calculated from the magnetic dipole−dipole interaction may be caused by the exchange contribution, since D_{zz}(exchange) should be parallel to g_{zz}.[28]

Synthesis and Characterization of Ni^{II}(OEFB). Transmetalation of magnesium octaethylformylbiliverdin with $Ni^{II}(OAc)_2\cdot 4H_2O$ produces nickel(II)(octaethylformylbiliverdin), Ni^{II}(OEFB), in ca. 29% yield. The black solid is soluble in aromatic and chlorinated solvents to produce brown-green solutions when concentrated and brown-yellow solutions when diluted. The solid is insoluble in *n*-hexane. The solid and solutions of Ni^{II}(OEFB) are air and light stable. The electronic spectrum of Ni^{II}(OEFB) in methylene chloride is shown in trace B of Figure 1.

The ^{1}H NMR spectrum of Ni^{II}(OEFB) shows features that are typical for a diamagnetic complex, but the spectrum suffers from poor dispersion at 300 MHz. The methyl resonances are located in the 0.95−1.45 ppm range, while the diastereotopic methylene resonances are located from 2.06 to 3.06 ppm. The four resonances from the formyl and meso protons are clearly resolved between 6.7 and 9.1 ppm and are shown in trace A of Figure 8. The ^{1}H resonance at 9.03 ppm was assigned to the formyl group in two ways. The ^{13}C NMR spectrum of the complex was obtained, and the chemical shift of the formyl carbon was found to be 183.7 ppm. Selected ^{1}H decoupling indicated that the proton with a resonance at 9.03 ppm was coupled to the formyl carbon atom. Furthermore, the addition of 0.28 equiv of the lanthanide shift reagent {tris(6,6,7,7,8,8,8-heptafluoro-2,2-dimethyl-3,5-octanedionato)europium(III)}, $Eu^{III}(FOD)_3$, to a methylene chloride-d_2 solution of Ni^{II}(OEFB) at 22 °C results in a large $\Delta\delta$ for the ^{1}H resonance at 9.03 ppm as seen in trace B of Figure 8. Thus both experiments are consistent with the assignment of the resonance at 9.03 to the formyl proton.

Further information on the helical nature of Ni^{II}(OEFB) has been obtained by titration of the chiral lanthanide shift reagent, {tris(3-(trifluoromethylhydroxymethylene)-*d*-camphorato)europium(III)}, $Eu^{III}(TFC)_3$, into a methylene chloride-d_2 solution of Ni^{II}(OEFB) at 22 °C. Trace C of Figure 8 shows the results of the addition of 1.7 equiv of $Eu^{III}(TFC)_3$ to Ni^{II}(OEFB). Each

(24) Chikira, M.; Kon, H.; Hawley, R. A.; Smith, K. M. *J. Chem. Soc., Dalton* **1979**, 245. Boyd, P. D. W.; Smith, T. D.; Price, J. H.; Pilbrow, J. R. *J. Chem. Phys.* **1972**, *56*, 1253. Boas, J. F.; Pilbrow, J. R.; Smith, T. D. *J. Chem. Soc. (A)* **1969**, 721. MacCragh, A.; Storm, C. B.; Koski, W. S. *J. Am. Chem. Soc.* **1965**, *87*, 1470.

(25) Morton, J. R.; Preston, K. F. *J. Magn. Reson.* **1978**, *30*, 577.

(26) Kuska, H. A.; Rogers, M. T.; Drullinger, R. E. *J. Phys. Chem.* **1967**, *71*, 109.

(27) Smith, T. D.; Pilbrow, J. R. *Coord. Chem. Rev.* **1974**, *13*, 173.

(28) Bencini, A.; Gatteschi, D. In *Magnetostructural Correlations in Exchange Coupled Systems*; Gatteschi, D., Kahn, O., Willett, R. D., Eds.; D. Reidel; Dordrecht, The Netherlands, 1985. Ozarowski, A.; Reinen, D. *Inorg. Chem.* **1986**, *25*, 1704.

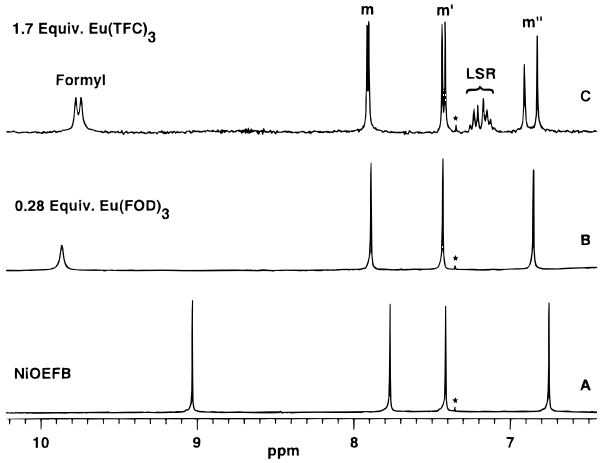

Figure 8. A, the downfield region of the 300 MHz ^{1}H NMR spectrum of Ni^{II}(OEFB) showing the formyl and meso protons. B, Ni^{II}(OEFB) and 0.28 equiv of the lanthanide shift reagent Eu(FOD)$_3$. C, Ni^{II}(OEFB) and 1.7 equiv of the chiral lanthanide shift reagent Eu(TFC)$_3$. The three spectra were collected at 22 °C in methylene chloride-d_2. An impurity is marked with *. Resonances from the lanthanide shift reagent (LSR) are marked. Meso protons are marked m, m′, and m″.

of the formyl and meso resonances of Ni^{II}(OEFB) have doubled as a result of forming a diastereomeric complex with the chiral lanthanide shift reagent. Each resonance in the split pairs of resonances is of equal integrated area. This indicates that either (1) the chiral lanthanide shift reagent does not bias the racemic mixture of the helical complex, Ni^{II}(OEFB), toward one enantiomer or (2) such biasing is impeded by a high barrier associated with M to P helix interconversion.

In both lanthanide shift reagent experiments, the formyl group is the site of lanthanide coordination to the helical nickel complex since this resonance shows the largest $\Delta\delta$. The variation observed in the difference in chemical shift of two enantiotopic resonances, caused by the addition of chiral Eu^{III}(TFC)$_3$, is due to the differing geometries of the two diastereomeric Eu^{III}(TFC)$_3$·Ni^{II}(OEFB) complexes formed.[29]

Synthesis and Characterization of Co^{II}(OEFB). Magnesium octaethylformylbiliverdin was transmetalated by Co^{II}(OAc)$_2$·4H$_2$O to produce cobalt(II)(octaethylformylbiliverdin), Co^{II}(OEFB), in reasonable yield (ca. 27%). The dark black solid decomposes in the presence of air over the span of several months. The solid is soluble in a range of chlorinated and aromatic solvents yielding brown-yellow solutions but is insoluble in nonpolar solvents such as *n*-hexane. The electronic absorption spectrum of Co^{II}(OEFB) in methylene chloride is shown in trace C of Figure 1. Solutions of Co^{II}(OEFB) quickly decompose in the presence of dioxygen and light or heat to produce several decomposition products. The major photooxidation product is currently under investigation.

Co^{II}(OEFB) is a low spin ($S = 1/2$) species, as established by magnetic susceptibility and EPR measurements (discussed later). The effective magnetic moment of Co^{II}(OEFB) at 22 °C in methylene chloride-d_2 is 1.7 μ_B.

Co^{II}(OEFB) has C_1 symmetry which results in a total of 28 anticipated ^{1}H NMR resonances (8 diastereotopic methylene pairs, 8 methyl, 3 meso, and 1 formyl resonance). To identify the meso and formyl resonances, a sample of Co^{II}(OEFB) selectively deuterated at the meso and formyl positions, Co^{II}(OEFB-meso/formyl-d_4), was synthesized by the photooxidation of Mg^{II}(OEP-meso-d_4) followed by transmetalation with Co^{II}(OAc)$_2$·4H$_2$O. The ^{2}H NMR spectrum of Co^{II}(OEFB-meso/formyl-d_4) in chloroform solution is shown in trace A of Figure 9, while the ^{1}H NMR spectrum of Co^{II}(OEFB) under identical conditions is shown in trace B. The ^{1}H and ^{2}H NMR chemical shifts do not correlate exactly due to the isotope effect.[30] Trace C is an expansion of the diamagnetic region of the ^{1}H NMR spectrum of Co^{II}(OEFB). The meso/formyl resonances are identified in the ^{1}H NMR spectra with * and were assigned based upon the ^{2}H NMR spectrum of Co^{II}(OEFB-meso/formyl-d_4) and ^{1}H T_1 and T_2^* relaxation constants. Within Figure 9, the methylene resonances have been labeled with the numerals 1−16, and the methyl resonances have been labeled with letters a−h. Although all 28 resonances are observed, specific assignment of the formyl proton resonance has not been determined. Addition of the lanthanide shift reagent Eu^{III}(FOD)$_3$ to a chloroform solution of Co^{II}(OEFB-meso/formyl-d_4) does not result in a significant shift of any of the ^{2}H resonances. The ^{2}H NMR resonance of the most downfield shifted meso/formyl shows a dramatic line width dependence upon temperature, while the other ^{2}H meso/formyl resonances do not. Below +20 °C the most downfield meso/formyl ^{2}H resonance broadens beyond detection. Based on the unique behavior of the most downfield resonance, it is reasonable to assign this resonance to the formyl deuteron.

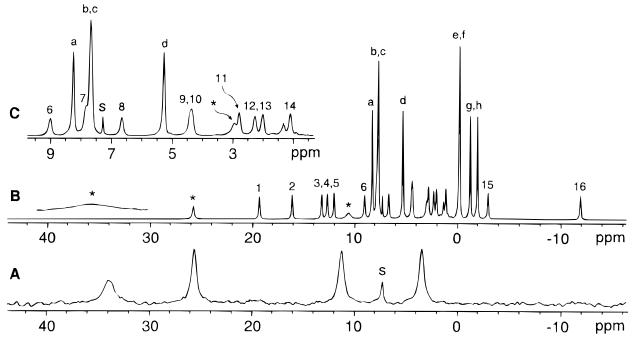

Figure 9. A, the 46 MHz ^{2}H NMR spectrum of Co^{II}(OEFB-meso/formyl-d_4) in chloroform at 40 °C. The residual ^{2}H resonance from chloroform is marked. B, the 300 MHz ^{1}H NMR spectrum of Co^{II}(OEFB) in chloroform-*d* at 40 °C. The spectrum between 30 and 40 ppm is shown expanded to highlight the most downfield meso/formyl resonance. C, expansion of the diamagnetic region of Co^{II}(OEFB) in chloroform-*d* at 40 °C. All resonance marked with * are assigned as those from the meso/formyl protons. The methylene resonances are labeled with the numerals 1−16 and the methyl resonances with letters a−h. The ^{1}H and ^{2}H NMR chemical shifts do not correlate exactly because of the isotope effect.

The methylene and methyl resonances can be assigned on the basis of relative integrated intensities and the magnitude COSY spectrum shown in Figure 10.[31] This spectrum also confirms the meso/formyl resonance assignments since these resonances do not have cross peaks. Within each ethyl group the diastereotopic methylene resonances have a cross peak between them, which indicates that they are a geminal pair, and an additional two cross peaks that indicate that these methylene protons are coupled to a methyl resonance.

The chemical shifts of all of the resonances of Co^{II}(OEFB) show a linear dependence upon T^{-1}, as expected for a simple, low spin ($S = 1/2$) formulation. Relevant data for the four meso/formyl resonances and the most downfield methylene pair of

(29) Sullivan, G. R. In *Topics in Stereochemistry*; Eliel, E. L., Allinger, N. L., Eds.; John Wiley and Sons, Inc.: New York, 1978; Vol. 10, p 287.

(30) Such sizable isotope effects are well-known in the ^{2}H NMR spectra of paramagnetic molecules. See: Horn, R. R.; Everett, G. W. *J. Am. Chem. Soc.* **1971**, *93*, 7173. Balch, A. L.; Chan, Y.-W.; La Mar, G. N.; Latos−Grażyński, L.; Renner, M. W. *Inorg. Chem.* **1985**, *24*, 1437.

(31) Keating, K. A.; de Ropp, J. S.; La Mar, G. N.; Balch, A. L.; Shiau, F. Y.; Smith, K. M. *Inorg. Chem.* **1991**, *30*, 3258.

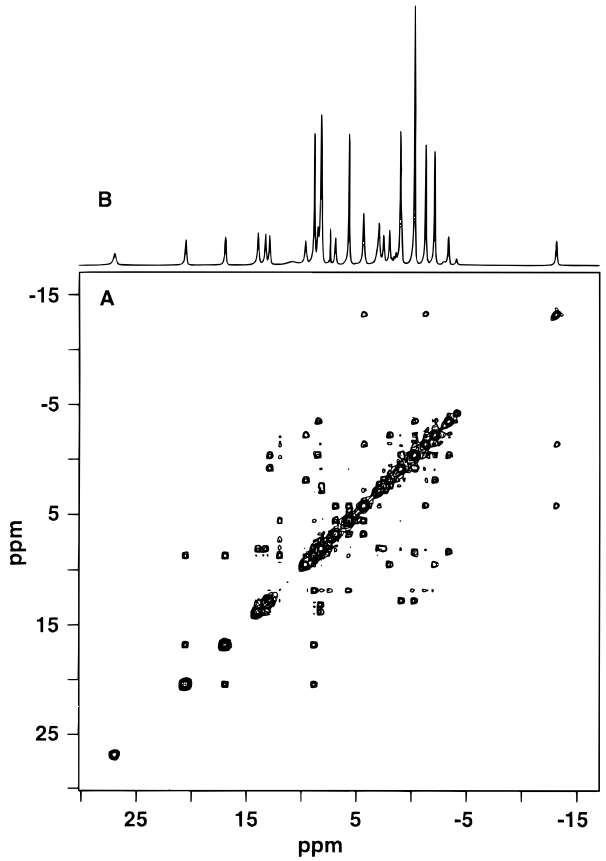

Figure 10. A, the 300 MHz ^{1}H NMR MCOSY of Co^{II}(OEFB) in chloroform-*d* at 23 °C. B, the reference ^{1}H spectrum.

resonances and the most upfield methylene resonance are given in the Supporting Information.

Preparation of the Cobalt Verdoheme Analogue, [Co^{II}(OEOP)]$^+$. The addition of hydrogen peroxide to a 1:1 methylene chloride:methanol solution of Co^{II}(OEFB) followed by anion metathesis with ammonium hexafluorophosphate and chromatography produced [Co^{II}(OEOP)](PF$_6$) in 26% yield. Unlike the oxidation of Cu^{II}(OEFB), no carbon monoxide was detected above the reaction solution. This reaction is highly solvent dependent, and it is essential that methanol be present. When the reaction is run in methylene chloride alone, oxidation yields the tetraethylpropentdyopent complex, Co^{II}(C$_{17}$H$_{21}$N$_2$O$_2$)$_2$, which has been characterized independently.[32] Both the UV/vis and ^{1}H NMR spectrum of the [Co^{II}(OEOP)](PF$_6$) complex produced are identical with that of an authentic sample.[23]

EPR Studies of Co^{II}(OEFB). The EPR spectrum of Co^{II}(OEFB) has been collected in both toluene and toluene/pyridine glasses at 15 K. The toluene glass of Co^{II}(OEFB) gave a poorly resolved EPR spectrum, while the dioxygen free toluene/pyridine (100:1 v/v) glass of Co^{II}(OEFB) at 15 K (trace A of Figure 11) shows ^{59}Co ($I = 7/2$) and ^{14}N ($I = 1$) hyperfine structure. Trace B of Figure 11 shows a simulation of this spectrum and was used to determine the following anisotropic *g*-values and ^{59}Co hyperfine coupling constants: $g_x = 2.181$, $g_y = 2.465$, $g_z = 2.001$, $A_x = 5.1 \times 10^{-4}$ cm^{-1}, $A_y = 52 \times 10^{-4}$ cm^{-1}, $A_z = 69 \times 10^{-4}$ cm^{-1}, A(N) $= 15 \times 10^{-4}$ cm^{-1}. This EPR spectrum is consistent with the formation of a five-coordinate pyridine adduct, (py)Co^{II}(OEFB), which is a typical, low-spin ($S = 1/2$) cobalt(II) complex.[33,34] Solutions of Co^{II}(OEFB) in toluene/pyridine (100:1 v/v) prepared under aerobic conditions form a dioxygen adduct, (py)Co^{II}(OEFB)(O$_2$). The EPR spectrum of the dioxygen adduct, under a dioxygen atmosphere, at 15 K is shown in trace C of Figure 11. Trace D is an expansion of this spectrum with a simulation shown in trace E. The simulation was used to determine the following anisotropic *g*-values and ^{59}Co hyperfine coupling constants: $g_x = 2.007$, $g_y = 1.988$, $g_z = 2.075$, $A_x = 10 \times 10^{-4}$ cm^{-1}, $A_y = 7.4 \times 10^{-4}$ cm^{-1}, $A_z = 15 \times 10^{-4}$ cm^{-1}. Samples prepared and sealed under a dioxygen atmosphere still show components of the EPR spectrum of unoxygenated (py)Co^{II}(OEFB). Dioxygen binding is reversible, since bubbling dinitrogen through the dioxygen-saturated solution restores the EPR spectrum of (py)Co^{II}(OEFB).

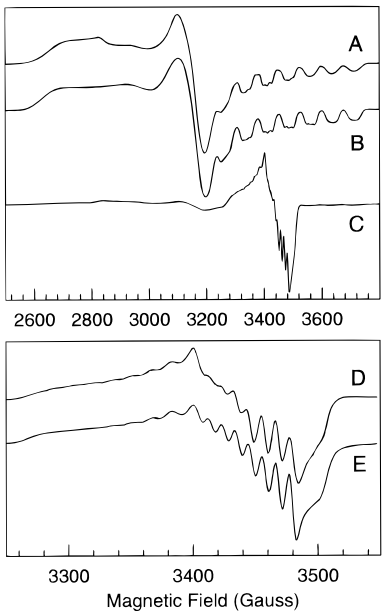

Figure 11. A, the X band EPR spectrum of a 3 mM dioxygen-free toluene/pyridine (100:1 v/v) glass of Co^{II}(OEFB) at 77 K. B, the simulation of the spectrum in trace A. C, the EPR spectrum of the dioxygen adduct (py)Co^{II}(OEFB)(O$_2$) at 77 K formed by the room-temperature addition of dioxygen gas to the dioxygen-free sample of Co^{II}(OEFB) in toluene/pyridine (100:1 v/v). D, an expansion of the spectrum in trace C. E, the simulation of the spectrum in trace D.

Electrochemical Studies. The electrochemical behavior of the three complexes of octaethylformylbiliverdin have been examined in methylene chloride. Figure 12 shows the cyclic voltammograms (CV) for Cu^{II}(OEFB) (trace A), Ni^{II}(OEFB) (trace B), and Co^{II}(OEFB) (trace C) in dioxygen-free methylene chloride with tetra(*n*-butyl)ammonium perchlorate as the supporting electrolyte. The behavior of each complex is similar. For each compound, there are two reversible reduction waves. The reduction potentials, which are collected in Table 4, show only modest variation within the series of compounds. Thus, the reductions may be largely ligand-localized. In addition to the two reductions, each complex shows evidence of an irreversible oxidation. The redox behavior of Co^{II}(OEFB) in dioxygen-free pyridine solution (see Table 4) shows a similar nonreversible oxidation ($E_f°$, vs [Fc/Fc$^+$]: −522 mV) and two reversible reductions at −1098 mV and −1689 mV ($E_f°$, vs [Fc/Fc$^+$]). Thus the electrochemical behavior of this complex shows a nearly negligible effect from pyridine coordination on the reductive processes.

(32) Koerner, R.; Olmstead, M. M.; Van Calcar, P. M.; Winkler, K.; Balch, A. L. *Inorg. Chem.*, in press. For information on the copper analogue, Cu(C$_{17}$H$_{21}$N$_2$O$_2$)$_2$, see ref 15.

(33) Walker, F. A. *J. Am. Chem. Soc.* **1970**, *92*, 4235.
(34) Walker, F. A. *J. Magn. Reson.* **1974**, *15*, 201.

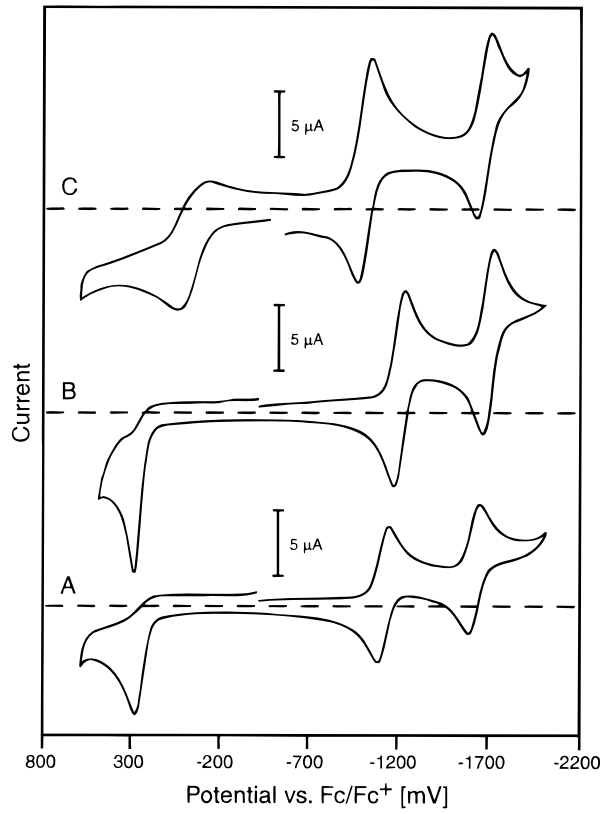

Figure 12. The cyclic voltammograms of (A) Cu^{II}(OEFB), (B) Ni^{II}(OEFB) and (C) Co^{II}(OEFB) in dioxygen-free methylene chloride with 0.1 M tetrabutylammonium perchlorate as the supporting electrolyte. The dashed line represents the zero of current.

Table 4. Electrochemical Data for Cu^{II}(OEFB), Ni^{II}(OEFB), and Co^{II}(OEFB)

	Cu^{II}OEFB	Ni^{II}OEFB	Co^{II}OEFB	
solvent	CH_2Cl_2	CH_2Cl_2	CH_2Cl_2	pyridine
concn (mM)	0.75	1.0	1.1	0.80
E_f vs [Fc/Fc$^+$] (mV)				
oxidation	268[a]	239[a]	35[a]	−522[a]
first redn	−1120	−1210	−1013	−1098
second redn	−1625	−1707	−1681	−1689
CV ΔE_p (mV)				
oxidation	ir[b]	ir[b]	170	190
first redn	58	60	82	76
second redn	58	58	78	84
OSWV $W_{1/2}$ (mV)				
oxidation	150	147	175	135
first redn	117	117	135	130
second redn	116	120	138	128

[a] Determined from the peak potential of the Osteryoung Square Wave Voltammogram. [b] ir: not determined because of the irreversible nature of this electrochemical process.

Discussion

Since we experienced difficulties in obtaining iron complexes of octaethylformylbiliverdin, we turned to the preparation of the more stable complexes of copper(II), nickel(II), and cobalt(II) as models to examine fundamental aspects of the coordination by this ligand. The available data indicate that octaethylformylbiliverdin forms mononuclear, four-coordinate MN_4 complexes with Cu(II), Ni(II), and Co(II) in which the metal coordination is distorted somewhat from planarity as is seen in the crystal structure of the copper complex. There appear to be considerable structural similarities between these complexes, Cu^{II}(OEFB), Ni^{II}(OEFB), and Co^{II}(OEFB), and those of octaethylbiliverdin, Cu(OEB), Ni(OEB), and Co(OEB). In each case, the ligand forms a helical unit in which the two end groups on the tetrapyrrole overlap one another. These ligands cannot be planar if they are to accommodate the M−N bond lengths for first row, late transition metal ions, and the van der Waals radii of the terminal groups on the tetrapyrrole ligand. For this set of complexes, the metal ions have adopted coordination geometries that are distorted from planarity but are certainly not tetrahedral. Figure 4 shows the detailed comparison which has been made between the structures of Cu^{II}(OEFB) and Cu^{II}(OEB$^\bullet$).

Despite the structural similarities between the formylbiliverdin complexes and the biliverdin complexes, there are important differences in their electronic structures. Octaethylformylbiliverdin coordinates to these late, first-row transition metals as a simple dianion. In contrast, octaethylbiliverdin forms a trianion and can readily exist in multiple oxidation states. Thus, the formylbiliverdin ligand forms a series of neutral complexes with Cu(II), Ni(II), and Cu(II) that have spectroscopic and structural properties which are characteristic of typical, low-spin complexes.[35] In contrast, octaethylbiliverdin forms neutral complexes with copper, nickel, and cobalt that have remarkable electronic structures. All three are paramagnetic and involve some degree of the ligand radical state in their electronic structure. For example, the neutral copper complex is formulated as a copper(II) complex of the ligand radical dianion, Cu^{II}(OEB$^\bullet$).

These formylbiliverdin complexes also have a number of similarities to complexes of the porphyrins. With the three metal ions considered here, both ligands form neutral, low-spin complexes. Although the formylbiliverdin ligand is not able to present the opportunity for planar coordination that a porphyrin does, it does present a similar set of pyrrole donors and a similar dianionic charge on the entire ligand. The similarities between the two ligand systems are particularly striking in the case of cobalt(II) where both ligands yield complexes that bind pyridine and are capable of acting as reversible dioxygen carriers in the presence of an axial base.

The copper(II) verdoheme cation, $[Cu^{II}(OEOP)]^+$, much like copper(II) octaethylporphyrin,[24] dimerizes in frozen solution as demonstrated by low-temperature EPR. Calculation of the dipole−dipole component of the zero-field splitting tensor based upon the geometrical data taken from the X-ray crystal structure of $[Cu^{II}(OEOP)](PF_6)\cdot CH_2Cl_2$ shows that the structure in frozen solution is very similar to that in the crystalline state. The small difference between the experimentally measured values of D, E, and the g_{zz}-D_{zz} angle and those calculated based on the X-ray structure of the dimer is most likely due to a slight difference in the geometry of the $[Cu^{II}(OEOP)]^+$ dimer in frozen solution, the pattern of spin density delocalization, or the effect of the exchange contribution to the zero-field splitting. We expect the exchange contribution to the zero-field splitting to be small since there is no covalent interaction between the $[Cu^{II}(OEOP)]^+$ units in the dimer.

Finally, we have shown that it is possible to convert the formylbiliverdin complexes, Cu^{II}(OEFB) and Co^{II}(OEFB), into the verdoheme (5-oxaporphyrin) type complexes, $[Cu^{II}(OEOP)]^+$ and $[Co^{II}(OEOP)]^+$, under oxidative conditions. In the case of the copper complex, carbon monoxide is also a product of this reaction with either dioxygen or hydrogen peroxide as the

(35) A previous study reported that the nickel complex of octaethylformylbiliverdin contained a significant amount of a free radical species.[9] We detected an EPR signal from our preparation of NiII(OEFB) that resembled that of Ni(OEB), a plausible contaminant. Quantification of this signal with DPPH showed that the contamination was less than 2%.

oxidant. The occurrence of such a reaction, with 5-oxaporphyrin formation and carbon monoxide production, indicates that it is feasible for formylbiliverdin complexes, under certain circumstances, to be intermediates in the transformation of porphyrins into verdohemes. Additionally, formylbiliverdin has been reported as the product of some heme degrading systems.[5]

Experimental Section

Preparation of Compounds. Cu^{II}(OEFB). Mg^{II}(OEP) (210 mg, 0.38 mmol) and anhydrous sodium sulfate (30 g) were added to 1.5 L of methylene chloride and was vigorously stirred under air while illuminated by a 750 W projector lamp placed 30 cm from the reaction vessel. After ca. 3 h of irradiation the solution was evaporated to dryness under reduced pressure. The resulting solid was dissolved in benzene (200 mL) and filtered to remove the sodium sulfate. $Cu^{II}(OAc)_2 \cdot H_2O$ (150 mg, 0.75 mmol) in 20 mL of methanol was added to the solution which was then brought to reflux and stirred for 10 min. The solution was evaporated to dryness under reduced pressure, redissolved in benzene, and chromatographed on silica gel (4 × 15 cm). Benzene eluted a fast moving red band which was identified as H_2OEP by its UV/vis spectrum. At this point, the eluant was switched to 2% methanol in benzene to elute Cu^{II}(OEFB) as a brown-orange solution. Cu^{II}(OEFB) was recrystallized from benzene/*n*-hexane. Yield 46.7 mg, 22%.

$[Cu^{II}(OEOP)]^+$ from Cu^{II}(OEFB). Dioxygen as Oxidant. A 3.6 mg portion of Cu^{II}(OEFB) was placed in a 50 mL Schlenk tube, and 10 mL of toluene was added to produce a brown-yellow solution. After the addition of 1 mL of trifluoroacetic acid, the Schlenk tube was flushed with dioxygen gas and sealed. The sealed reaction vessel was heated to 70 °C in an oil bath behind a safety shield. Heating for 17 h produced a dark green solution. Both carbon monoxide and carbon dioxide were detected in the headspace above the reaction solution by infrared spectroscopy of the gases (carbon dioxide by the asymmetric stretch at 2340 cm^{-1} and carbon monoxide by the P & R branches centered at 2143 cm^{-1}). The green reaction solution was evaporated to dryness, and the residue was dissolved in chloroform and was subjected to chromatography on silica gel (2 × 4 cm). Elution with chloroform removed a brown-orange band that contained unreacted Cu^{II}(OEFB). Continued elution with 15% methanol in chloroform produced a green band which was collected and evaporated to dryness to give the product as a green-black solid, formulated as $[Cu^{II}(OEOP)](CF_3CO_2)$: yield 2.3 mg, 56%. UV/vis spectrum: λ_{max}, nm: 400, 510, 546, 622, 666. A chloroform-*d* solution of the complex exhibited a ^{19}F NMR resonance at 76.3 ppm due to the trifluoroacetate anion.

Hydrogen Peroxide as Oxidant. A 50:50 mixture (50 μL) of 30% hydrogen peroxide and methanol was added to a solution of 5.8 mg (0.0092 mmol) of Cu^{II}(OEFB) in 100 mL of methylene chloride and allowed to stand at room temperature. After 2 h the blue-green solution was evaporated to dryness under reduced pressure. The dark green solid was redissolved in 10 mL of methylene chloride, and 1 mL of a saturated methanol solution of ammonium hexafluorophosphate was added. The solution was evaporated to dryness, redissolved in a minimum volume of methylene chloride, filtered and chromatographed on silica gel. The blue-green band was eluted with 10% methanol in methylene chloride, evaporated to dryness, and placed under a vacuum. Yield: 5.8 mg (84%) as $[Cu^{II}(OEOP)](PF_6)$. UV/vis spectrum: λ_{max}, nm: 398, 510, 546, 622, 666.

$[Cu^{II}(OEOP)](PF_6)$ from Cu^{II}(OEP). A 10 mL aqueous solution of 30% hydrogen peroxide (large molar excess) was added to a solution of 100.3 mg (0.17 mmol) of Cu^{II}(OEP) in 75 mL of a methylene chloride. The biphasic solution was allowed to stand for 16 h with venting to allow release of the gas produced. The pink solution slowly turned muddy green. The mixture was diluted with an additional 50 mL of methylene chloride and washed several times with water. The organic layer was evaporated to dryness under vacuum, and the residue was dissolved in chloroform. The chloroform solution was subjected to chromatography on silica gel (2.5 × 15 cm column) with elution with chloroform to remove several unidentified nonpolar products. Subsequent elution with chloroform containing 10% methanol produced a blue-green fraction that contained $[Cu^{II}(OEOP)]^+$. This polar product was dried under vacuum, redissolved in 15 mL of methylene chloride, and then mixed with a saturated solution of ammonium hexafluorophosphate in 15 mL of methanol. This mixture was stirred for 5 min, and then the residual white precipitate was removed by filtration. The solvent was again removed under vacuum, the blue solid was dissolved in a minimum volume of methylene chloride and crystallized by slow diffusion of methanol to give 2.3 mg (2% yield) of $[Cu^{II}(OEOP)](PF_6)$. No attempt was made to optimize the yield of $[Cu^{II}(OEOP)](PF_6)$, but addition of only a stoichiometric equivalent of 30% hydrogen peroxide resulted in essentially no reaction over the course of 1 week. UV/vis (in methylene chloride), λ_{max}, nm (ϵ, M^{-1} cm^{-1}): 398 (7800) 510 (1700) 546 (1900) 622 sh (2100) 666 (5000). IR (solid), (cm^{-1}): 1739m, 1602w, 1464m, 1378w, 1275m, 1122m, 1073m, 1014w, 957w, 742w.

Ni^{II}(OEFB). Mg^{II}(OEP) (70 mg, 0.13 mmol) and anhydrous sodium sulfate (30 g) were added to 1.5 L of methylene chloride, and the solution was vigorously stirred under air while illuminated by a 750 W projector lamp placed 30 cm from the reaction vessel. After ca. 2 h of irradiation the solution was evaporated to dryness under reduced pressure. The resulting solid was dissolved in benzene (200 mL) and filtered to remove the sodium sulfate. $Ni^{II}(OAc)_2 \cdot 4H_2O$ (100 mg, 0.40 mmol) in 20 mL of methanol was added to the solution which was then brought to reflux and stirred for 10 min. The solution was evaporated to dryness under reduced pressure, redissolved in benzene, and chromatographed on silica gel (4 × 15 cm). Benzene eluted a fast moving red band which was identified as H_2OEP by UV/vis. At this point, the eluant was switched to 2% methanol in benzene to elute Ni^{II}(OEFB) as a brown-green solution. Ni^{II}(OEFB) was recrystallized from benzene/*n*-hexane: yield, 23.1 mg (29%). EI-MS *m*/*z* (rel intensity): 622.28 (8) M^+, 593.28 (100) $[M - CHO]^+$.

Co^{II}(OEFB). Mg^{II}(OEP) (111.7 mg, 0.20 mmol) and anhydrous sodium sulfate (30 g) were added to 1.5 L of methylene chloride, and the solution was vigorously stirred under air while illuminated by a 750 W projector lamp placed 30 cm from the reaction vessel. After ca. 2 h of irradiation, $Co^{II}(OAc)_2 \cdot 4H_2O$ (75 mg, 0.3 mmol) in 10 mL of methanol was added to the solution which was then stirred and evaporated to dryness under reduced pressure. The resulting solid was dissolved in benzene, filtered to remove the sodium sulfate, and chromatographed on silica gel (4 × 15 cm) with benzene to elute a fast moving red band which was identified as H_2OEP by UV/vis. At this point, the eluant was switched to 2% methanol in benzene to elute Co^{II}(OEFB) as a brown-yellow solution. Co^{II}(OEFB) was recrystallized from benzene/*n*-hexane: yield, 34.0 mg (27%). EI-MS *m*/*z* (rel intensity): 623.28 (16) M^+, 594.28 (100) $[M - CHO]^+$. Anal. Calcd for $C_{36}H_{44}O_2N_4Co$: C, 69.33; H, 7.11; N, 8.98. Found: C, 69.48; H, 7.34; N, 9.06.

Co^{II}(OEFB-meso/formyl-d_4). Co^{II}(OEFB-meso/formyl-d_4) was prepared as above, except Mg^{II}(OEP-meso-d_4) was used.

$[Co^{II}(OEOP)](PF_6)$ from Co^{II}(OEFB). Dilute hydrogen peroxide (240 μL, 10 μL 30% H_2O_2 in 5 mL of methanol) was slowly added to a 1:1 methylene chloride:methanol solution of Co^{II}(OEFB) (5.2 mg, 0.0083 mmol). The resulting green solution was treated with 1 mL of a saturated solution of ammonium hexafluorophosphate in methanol and evaporated to dryness under reduced pressure. The dark solid was redissolved in a minimal volume of methylene chloride and subjected to chromatography on silica gel (2 × 5 cm). The desired product, $[Co^{II}(OEOP)](PF_6)$, eluted as a blue band with 1% methanol in methylene chloride and was evaporated to dryness and placed under a vacuum. Yield: 1.6 mg (26%).

EPR Simulation for Dimeric $[Cu^{II}(OEOP)]^+$. A program was written that simulates the triplet spectrum utilizing the following spin Hamiltonian

$$\boldsymbol{H} = \beta \mathbf{H}\cdot\mathbf{g}\cdot\mathbf{S} + D\{\mathbf{S}_z^2 - (1/3)\,S(S+1)\} + E(\mathbf{S}_x^2 - \mathbf{S}_y^2)$$

and was solved exactly as discussed elsewhere.[36] The hyperfine term $\mathbf{S}\cdot\mathbf{A}\cdot\mathbf{I}$ was then treated as a first-order perturbation. Hyperfine tensor, **A**, was assumed to be parallel to the **g** tensor but the zero-field splitting tensor, **D**, was allowed to have its main axes rotated versus those of **g**.

(36) Baranowski, J.; Cukierda, T.; Jezowska-Trzebiatowska, B.; Kozlowski, H. *Chem. Phys. Lett.* **1976**, *39*, 606.

Table 5. Crystallographic Data for Cu^{II}(OEFB) and $[Cu^{II}(OEOP)](PF_6)\cdot CH_2Cl_2$

	Cu^{II}(OEFB)	$[Cu^{II}(OEOP)](PF_6)\cdot CH_2Cl_2$
formula	$C_{36}H_{44}CuN_4O_2$	$C_{36}H_{45}Cl_2CuF_6N_4OP$
formula wt ($g\cdot mol^{-1}$)	628.29	829.17
color and habit	red prism	red needle
crystal system	triclinic	triclinic
space group	$P\bar{1}$	$P\bar{1}$
a, Å	12.492(2)	11.0442(15)
b, Å	15.007(2)	14.080(2)
c, Å	28.059(4)	14.1336(13)
α, deg	83.830(10)	104.666(9)
β, deg	86.030(10)	101.707(9)
γ, deg	68.080(10)	110.542(10)
V, $Å^3$	4849.2(12)	1884.9(4)
Z	6	2
T, K	130	130
d_{calcd}, $g\cdot cm^{-3}$	1.291	1.461
radiation, (*λ* Å)	CuK_α 1.54178	CuK_α 1.54178
μ, mm^{-1}	1.242	3.086
range of transmission factors	0.70−0.81	0.71−0.89
R1[a]	0.0434	0.0410
wR2[b]	0.1106	0.0838

[a] $R1 = \sum||F_o| - |F_c||/\sum|F_o|$. [b] $wR2 = [\sum[w(F_o^2 - F_c^2)^2]/\sum[w(F_o^2)]]^{1/2}$.

Since no deviation of **g** from axial symmetry was detected, only the rotation of **D** versus **g** in the *xz* plane is relevant.

The zero-field tensor components were calculated based upon an expression that takes into account a centrosymmetric dimer and electron delocalization onto the ligand:[27]

$$D_{\alpha\gamma}^{dipole} = \frac{\mu_B^2}{2}\sum_i\sum_j g_\alpha g_\gamma(\delta_{\alpha\gamma} - 3\sigma_\alpha\sigma_\gamma)\rho_i\rho_j r_{ij}^{-3}$$

The summation runs over all sites carrying spin density in each of the interacting monomers. The parameters g_α, g_γ indicate g_x, g_y or g_z, $\delta_{\alpha\gamma}$ is the Kronecker's delta, r_{ij} is the distance between site "*i*" in one monomer and site "*j*" in the other monomer, σ_α, σ_γ are the cosines of the angle between the directions of the *g* components and the vector r_{ij}, ρ_i is the spin density on site "*i*", and ρ_j is the spin density on site "*j*". The resulting tensor **D** is then diagonalized and parameters *D* and *E* of the spin Hamiltonian are calculated as

$$D = (2D_{zz} - D_{xx} - D_{yy})/2$$

$$E = (D_{xx} - D_{yy})/2$$

X-ray Data Collection for Cu^{II}(OEFB) and $[Cu^{II}(OEOP)](PF_6)\cdot CH_2Cl_2$. A red prism of Cu^{II}(OEFB) was obtained by the slow diffusion of *n*-hexane into a benzene solution of Cu^{II}(OEFB). A red needle of $[Cu^{II}(OEOP)](PF_6)\cdot CH_2Cl_2$ was obtained by the slow diffusion of methanol into a methylene chloride solution of $[Cu^{II}(OEOP)](PF_6)$. The datum crystals were coated with a light hydrocarbon oil and mounted in the 130 K dinitrogen stream of a Siemens P4 rotating anode diffractometer equipped with a low-temperature device. Crystal data and data collection parameters are given in Table 5. Two check reflections showed less than a 2% decay during the data collection. The data were corrected for Lorentz and polarization effects.

Solution and refinement for Cu^{II}(OEFB) and $[Cu^{II}(OEOP)](PF_6)\cdot CH_2Cl_2$. Calculations were performed with the SHELXTL v5.03 suite of programs for the Cu^{II}(OEFB) data set, while calculation for $[Cu^{II}(OEOP)](PF_6)\cdot CH_2Cl_2$ were performed with SHELXTL-97. Scattering factors for neutral atoms and corrections for anomalous dispersion were taken from a standard source.[37] An absorption correction was applied to the data.[38] The initial solution of both structures were obtained by direct methods. Hydrogen atoms were found on a difference map and refined at ideal geometries. The structure of Cu^{II}(OEFB) shows disorder in the position of one methyl group, C(94). This was modeled with the disordered methyl group in two sites, C(94) and C(94A) (not shown), with occupancies which refined to 0.59 and 0.41, respectively. Within the structure of $[Cu^{II}(OEOP)](PF_6)\cdot CH_2Cl_2$, the oxygen atom is site-disordered with respect to the carbon atoms that occupy the same meso position at two different, "trans"-related sites. Atoms O/C20A and C10/O10A refined to occupancies of 0.919(10)/0.081(10) for the two atoms at the same site. The structure of $[Cu^{II}(OEOP)](PF_6)\cdot CH_2Cl_2$ was found to be isostructural with that of $[Co^{II}(OEOP)](PF_6)\cdot CH_2Cl_2$.[23] The complete table of atomic positional parameters and a full table of bond lengths and angles for both data sets have been placed in the Supporting Information.

Instrumentation. ^1H NMR spectra were recorded on a General Electric QE−300 FT NMR operating in the quadrature mode (^1H frequency is 300 MHz). Typical spectra were collected over a 30 kHz spectral window with 8 K complex points, 256−2048 transients, and a repetition rate of 2.5 transients/s. The signal-to-noise ratio was improved by apodization of the free induction decay. The residual ^1H resonances of the deuterated solvents were used as secondary references.

The ^2H NMR spectra were recorded on a General Electric QE−300 operating at 46 MHz. Typical spectra were recorded over a 4 kHz spectral window with 2 K complex points, 512−2048 transients, and a repetition rate of 1.6 transients/s. The signal-to-noise ratio was improved by apodization of the free induction decay. Spectra were referenced to the residual ^2H NMR resonance of the solvent used.

The MCOSY spectrum was obtained after collection of a ref 1D spectrum. The 2D spectrum was collected over a 30 kHz spectral window (to include all resonances) with 1 K complex points in t_2 and 512 t_1 increments of 256 transients each. Eight dummy scans were performed prior to the collection of the first block. The resulting data were zero filled to 1K × 1K complex points and apodized in both dimensions by an unshifted sinebell squared function prior to Fourier transformation and symmeterization.

Electrochemical measurements were recorded on a BioAnalytical Systems CV-50W potentiostat. All measurements were conducted at room temperature under an argon atmosphere using 0.1 M tetrabutylammonium perchlorate as the supporting electrolyte, a gold disk (0.75 mm radius) working electrode, Ag/Ag^+ reference electrode, and a platinum foil auxiliary electrode. Cyclic voltammograms were collected with a 100 or 200 mV/s sweep rate. Osteryoung square wave voltammograms were collected using a 25 mV sweep width amplitude, 15 Hz sweep width frequency, 4 mV step potential, and a 2 s quiet time.

Absorption spectra were recorded on an OLIS/Cary-17 spectrophotometer or a Hewlet-Packard 8452A diode array spectrophotometer. EPR spectra were recorded in the X band on a Bruker ECS-106 spectrometer equipped with an Oxford helium cryostat. Typical spectra were collected using a 2 G modulation amplitude and a 300 s time constant. High-resolution EI (70 eV) mass spectrometry was performed on a VG Analytical ZAB-2F−HS mass spectrometer. Elemental analysis was performed by Midwest Microlab, Indianapolis, IN. Magnetic susceptibilities were determined by the Evans technique.[39]

Acknowledgment. We wish to thank the National Institutes of Health (GM-26226) for financial support.

Supporting Information Available: Tables of all atomic positional parameters, bond lengths, bond angles, anisotropic thermal parameters, hydrogen atom positions, and data collection parameters for Cu^{II}(OEFB) and $[Cu^{II}(OEOP)](PF_6)$ and Curie plots of chemical shift versus T^{-1} for Co^{II}(OEFB) (34 pages). See any current masthead page for ordering and Internet access instructions.

JA973088Y

(37) *International Tables for X-ray Crystallography*; Kynoch Press: Birmingham, England, 1974; Vol. 4.

(38) Parkins, S.; Moezzi, B.; Hope, H. *J. Appl. Crystallogr.* **1995**, *28*, 53.

(39) Evans, D. F.; James, T. A. *J. Chem. Soc., Dalton Trans.* **1979**, 723.